

Evolution of circuit complexity in a harmonic chain under multiple quenches

Kuntal Pal,^{*} Kunal Pal,[†] Ankit Gill,[‡] and Tapobrata Sarkar[§]

Department of Physics, Indian Institute of Technology, Kanpur 208016, India

Abstract

We study Nielsen's circuit complexity in a periodic harmonic oscillator chain, under single and multiple quenches. In a multiple quench scenario, it is shown that the complexity shows remarkably different behaviour compared to the other information theoretic measures, such as the entanglement entropy. In particular, after two successive quenches, when the frequency returns to its initial value, there is a lower limit of complexity, which cannot be made to approach zero. Further, we show that by applying a large number of successive quenches, the complexity of the time evolved state can be increased to a high value, which is not possible by applying a single quench. This model also exhibits the interesting phenomenon of crossover of complexities between two successive quenches performed at different times.

arXiv:2206.03366v1 [quant-ph] 7 Jun 2022

^{*} kuntal@iitk.ac.in

[†] kunalpal@iitk.ac.in

[‡] ankitgill20@iitk.ac.in

[§] tapo@iitk.ac.in

I. INTRODUCTION

Nonequilibrium dynamics of quantum systems after a quench of the system parameters is paradigmatic of the current thrust in research on quantum information theory, and is expected to be of fundamental importance in technological applications of quantum theory. While there is a large number of ways to take a system out of equilibrium and then study its evolution, quantum quenches are ubiquitous in this regard and have played a vital role in our understanding of nonequilibrium dynamics of closed quantum systems [1]. Here, the final fate of the system depends on its integrable or chaotic nature, and various physical measures have been used to characterise such a final state [2]. To this end, the reduced density matrix, entanglement measures calculated from the reduced density matrix, such as entanglement entropy (EE), entanglement negativity etc., as well as information theoretic quantities like mutual information have been widely used to study thermodynamic equilibrium after a quench [3]-[6].

On the other hand, it is essential to understand how information spreads across all the degrees of freedom of a many body system after the dynamical equilibrium of the system has been disturbed, and this seems to strongly depend on the integrable properties of the Hamiltonian. The notion of information scrambling, which is roughly the fact that any local perturbation will not be strictly local during the course of time evolution and can only be measured globally, is generally ascribed to chaotic systems. The canonical prescription to see the effect of scrambling, namely the out of time ordered correlator (OTOC) has been studied in a variety of systems mainly by using numerical methods [7]-[13]. Even though the general consensus is that the saturation of OTOC at late times indicate scrambling of information in chaotic systems, there are also results in the literature that point to the contrary. Among the significant ones, it was shown in [14], by means of computing OTOC (in an integrable Ising chain), and in [6] by computing the algebraic decay of mutual information (in spin $\frac{1}{2}$ chain), that integrable models also can show information scrambling. The authors of [15], on the other hand proved that OTOC of integrable systems that have unstable fixed points in phase space, can also show scrambling, therefore the notion of scrambling may not always be synonymous of chaos. To further support this point, one has to only point out that even a trivially integrable system like a collection of interacting simple harmonic oscillators gives a saturation of OTOC under a multiple quench protocol [16].

In the view of above discussion, in this paper our focus will be to study a relatively new information theoretic quantity, the circuit complexity (CC), in integrable systems that shows scrambling under multiple quenches. The notion of CC, that measures the number of gates it is required to create a desired target state starting from a given reference state, has recently gained a widespread attention in literature, specially because it can offer a probe to the black hole interiors. On the quantum mechanical side, the most popular method of quantifying the CC is due to Nielsen and collaborators [17]-[19], who developed a geometrical formulation on the space unitary operators to calculate the circuit complexity. The Nielsen complexity (NC), that measures the geodesic distance between two points on the unitary Riemannian manifold for a particular cost functional, was used in [20]-[24] for possible extensions in quantum field theories. The time evolution of NC after a quantum quench in integrable systems as studied in [25], shows linear growth followed by saturation, which generically captures the underlying physics of

the system. Quench in the context of complexity have been also studied in [26], [27]. On the other hand, with a slightly different motivation, the complexity between a reference state and the target state obtained by forward time evolution with a particular Hamiltonian followed by backward evolution with slightly different Hamiltonian shows markedly different behaviour, depending on whether the classical Hamiltonian is chaotic or not [29]. For a classically exactly solvable model such as a collection of harmonic oscillators, the complexity shows usual oscillatory behaviour, but for a classically chaotic system like the inverted harmonic oscillator, the complexity shows linear growth after some time, thereby making CC a good measure of the dynamics of the quantum chaotic system [29], [30]. Here we study the CC of interacting harmonic chain, which in terms of dynamics lies somewhat in between the above mentioned two examples of simple integrable systems and a fully chaotic system, as this integrable model we consider shows scrambling of information between different degrees of freedom [16]. The evolution of complexity is studied both under a single and the above mentioned multiple quench protocols. Our motivation here is two fold. Firstly, we want to study how a complicated measure like CC, which depends on the reference state, the target state, as well as on the cost functional chosen, behaves in multiple quench scenario and its comparison with the EE. To be specific, it is interesting to ask if the employment of more than one quenches can change the saturation time scales of EE and CC, as it has already been observed that the EE can saturate slowly compared to CC in a single quench scenario [31]. Our second aim is to see how CC of the full system behaves after the local information has already been distributed across the whole system, which in principle is encoded in the wave function. As the final state of this system points to a relaxation behaviour from the analysis of momentum distribution and EE, it is useful to see if the analysis of CC also gives the same conclusion. Our method is fully analytical and can be generalised for arbitrary time-dependent frequency and interaction strength profile of the harmonic chain.

The main results that we obtain here are as follows. For a single quench, we find that as expected, complexity shows revivals, whose time periods depend on the post-quench frequency of the oscillators. Indeed, dynamically generated time scales are responsible for these quasi revivals. Further, when such a quench is critical, the complexity grows at large times because of the logarithmic divergence of the zero mode contribution at this limit. Finally, when the zero mode contribution is subtracted from the complexity, it does not show any decoherence in time, which is contrary to what is observed in the same system, when the covariance matrix is used to calculate the complexity [32, 33].

For multiple quenches, we find that, unlike the entanglement entropy, the complexity does not attain a steady state value even after multiple quenches, but rather continues to oscillates even at large times. Further, after two successive quenches, when the reference state frequency goes back to initial value, the complexity has a finite value which is higher than the complexity just after the next quench. There is a limit on how close a time evolved state can be closer to the reference state before the quench, and complexity can not be made to approach close to zero by increasing the frequency, which controls its magnitude. In this regard, we find a novel phenomenon which is not possible to observe with a single quench, namely a quench performed at an earlier time (i.e., a quench with lower quench number i) ‘pushes away’ the time evolved target state far away on the space of unitaries compared to a quench performed at a later time. Hence there is a crossover of complexities of successive quenches just after the

$(i+1)$ th quench. Also, by using a sufficiently large number of quenches, a target state with large complexity can be prepared, which is in contrast with the single quench where the peaks of the complexity maxima are fixed by the quench frequency. These results are elaborated upon in the following sections.

II. COMPLEXITY EVOLUTION IN A HARMONIC CHAIN UNDER A SINGLE QUENCH

We consider a chain containing N mutually interacting harmonic oscillators (“harmonic chain”) whose frequency depends on time. Furthermore, the interaction strength is also assumed to be dependent on time. We will study the time evolution of Nielsen’s circuit complexity of such a system, when the system parameters, namely the frequency and the interaction strengths are quenched to different values under some definite protocols, which we will define in sequel. Complexity evolution of such a systems under a global quench has been studied in [33] using the covariance matrix method [32]. Here we shall employ the wavefunction method of calculating the circuit complexity, and use the solution of the Ermakov-Milne-Pinney (EMP) equation to write down the corresponding complexity. We will also discuss the differences in the resulting complexity computed using these two methods.

A. Ground state of the harmonic chain

The Hamiltonian under consideration is that of N mutually interacting harmonic oscillators whose frequency and interaction strength are explicit functions of time, and is given as

$$H(x_j, p_j, t) = \frac{1}{2} \left[\sum_{j=1}^N \left(p_j^2 + \omega(t)^2 x_j^2 \right) + k(t) \left(x_j - x_{j+1} \right)^2 \right] = \frac{1}{2} \left[\sum_{j=1}^N \left(p_j^2 + X^T \cdot K(t) \cdot X \right) \right]. \quad (1)$$

Here $X = (x_1, x_2, \dots, x_N)^T$ is a column matrix for the collective position of each oscillator, and K is a real symmetric matrix whose eigenvalues are denoted as λ_j . It is assumed that periodic boundary conditions are imposed on the chain.

By using an orthogonal transformation U , we can diagonalise the above Hamiltonian so that each of the N oscillators become decoupled. Denoting $Y = (y_1, y_2, \dots, y_N)^T = UX$ as the new coordinates and $K^D = UKU^T$ as the diagonal form of the matrix K , the transformed Hamiltonian can be written as

$$H^D(y_j, P_j, t) = \frac{1}{2} \left[\sum_{j=1}^N \left(P_j^2 + K_{jj}^D(t) y_j^2 \right) \right]. \quad (2)$$

We are interested in the ground state of the system. Since the Hamiltonian is an explicit function of time, hence to find the ground state of the system we can use the Lewis-Risenfeld theory of time-dependent invariant operators. In diagonal coordinates y_j , the ground state wavefunction corresponding to the Hamiltonian of Eq. (2) can be written as [34]

$$\Psi_0(y_j, t) = \left(\prod_{j=1}^N \frac{1}{b_j^2(t)} \det \frac{\sqrt{K^D(t)}}{\pi} \right)^{1/4} \exp \left[\sum_{j=1}^N \left(-\frac{1}{2} \Omega_j(t) y_j^2 + \alpha_j(t) \right) \right], \quad \Omega_j(t) = \frac{\sqrt{K_{jj}^D(t=0)}}{b_j^2(t)} - i \frac{\dot{b}_j(t)}{b_j(t)}. \quad (3)$$

Here $\alpha_j(t)$ is a time-dependent phase factor whose form will not be important to us, and an overdot indicates a derivative with respect to time. The auxiliary functions $b_j(t)$ satisfies the following EMP equation

$$\ddot{b}_j + \lambda_j(t)b_j - \frac{\lambda_j(0)}{b_j^3(t)} = 0, \quad (4)$$

where $\lambda_j(t) = \omega^2(t) + 2k(t)[1 - \cos(\frac{2\pi j}{N})]$, with $j = 1, 2, \dots, N$, are the time-dependent eigenvalues of the matrix K , and $\lambda_j(0) = \lambda_j(t=0)$. To determine the unknown constants appearing in the general solution of this equation, we need to impose conditions on it at some initial time, say $t = t_0$. Here, we shall impose the following conditions on $b(t)$ at the start of the quench $t = 0$:

$$b(t=0) = 1 \quad \text{and} \quad \dot{b}(t=0) = 0, \quad (5)$$

so that the wave function at $t = 0$ matches with that of the instantaneous harmonic oscillator at that instant of time. For a single time-dependent oscillator, this procedure has been used in [35] to find out the Nielsen complexity of the Lipkin-Meshkov-Glick model using the wave function method of [20],[28]. Recently, in [36] the solution of the EMP equation was also used to find out the complexity using the covariance matrix of a state and its comparison with the wavefunction method was also studied.

B. Nielsen complexity with the state at initial time as the reference

The quench protocol we consider is the following. We consider the chain containing N interacting oscillators with frequency ω_i and interaction strength k_i , and at time $t = 0$ we change these parameters to different constant values ω_f and k_f respectively. Our goal here is to find out the circuit complexity of the state at an arbitrary time $t > 0$ by taking the state at $t = 0$ to be the reference state. This reference state, being the product of ground states of N oscillators of frequency $\sqrt{\lambda_{j(in)}} = \sqrt{\lambda_j(t=0)}$, is also a Gaussian in the y_j coordinates, just like the target state. In such a case, the expression of the Nielsen complexity is well known and is given by [28]

$$\mathcal{C}(t) = \frac{1}{2} \sqrt{\sum_{j=1}^N (\mathcal{A}_j^2(t) + \mathcal{B}_j^2(t))}, \quad \mathcal{A}_j(t) = \ln \left(\frac{|\Omega_j|}{\sqrt{\lambda_j(0)}} \right), \quad \mathcal{B}_j(t) = \arctan \left(\frac{\text{Im}(\Omega_j)}{\text{Re}(\Omega_j)} \right). \quad (6)$$

With the form of $\Omega_j(t)$ given in Eq. (3), the expressions for the time dependent functions $\mathcal{A}_j(t)$ and $\mathcal{B}_j(t)$ can be written directly in terms of the auxiliary function $b_j(t)$ and its time derivative as [35]

$$\mathcal{A}_j(t) = \ln \left[\frac{\sqrt{b_j^2(t)\dot{b}_j^2(t) + \lambda_j(0)}}{\sqrt{\lambda_j(0)b_j^2(t)}} \right], \quad \mathcal{B}_j(t) = \arctan \left(\frac{b_j(t)\dot{b}_j(t)}{\sqrt{\lambda_j(0)}} \right). \quad (7)$$

Now to obtain these functions for the quench process considered here, we need the explicit solution of the auxiliary equation which satisfies the initial conditions of Eq. (5). To obtain the general solution of Eq. (4) with $\lambda_j(t)$ given above we follow the following procedure. We consider two linearly independent solutions of the classical equation of motion of the harmonic oscillator with frequency λ_j

$$\frac{d^2 g_j(t)}{dt^2} + \lambda_j g_j(t) = 0, \quad (8)$$

which we denote respectively as $g_{j1}(t)$ and $g_{j2}(t)$. Then a general solution of the corresponding auxiliary equation can be written as

$$b_j(t) = \sqrt{A_j g_{j1}^2(t) + 2B_j g_{j1}(t)g_{j2}(t) + C_j g_{j2}^2(t)}, \quad (9)$$

with the three consonants A_j, B_j, C_j are being related by the relation

$$A_j C_j - B_j^2 = \pm \frac{\lambda_j(0)}{W^2}, \quad (10)$$

where W the Wronskian of the two linearly independent classical solution. Any two independent constants, say, A_j and C_j can be obtained by using the conditions listed in Eq. (5) at $t = 0$.

For our case, since after the quench at $t = 0$ the frequency $\sqrt{\lambda_j}$ takes a constant value, the solution for the auxiliary equation can be written with $y = \sqrt{\lambda_j}t$ as

$$b_j(t) = \sqrt{A_j \cos^2 y + 2B_j \sin y \cos y + C_j \sin^2 y} = \sqrt{\alpha_j \cos(2y) + \beta_j \sin(2y) + \gamma_j}. \quad (11)$$

The relation between the two sets of constants can be worked out easily. Now, using the initial conditions and the relation of Eq. (10) between the three constants, we can obtain these constants to be

$$\alpha_j = \frac{\lambda_j - \lambda_j(0)}{2\lambda_j}, \quad \beta_j = 0, \quad \gamma_j = \frac{\lambda_j + \lambda_j(0)}{2\lambda_j}. \quad (12)$$

With this solution for the auxiliary function the exact expressions for the functions $\mathcal{A}_j(t)$ and $\mathcal{B}_j(t)$ are given by

$$\mathcal{A}_j(t) = \ln \left[\frac{\sqrt{\alpha_j^2 \lambda_j \sin^2(2y) + \lambda_j(0)}}{(\gamma_j + \alpha_j \cos(2y)) \sqrt{\lambda_j(0)}} \right], \quad \mathcal{B}_j(t) = \arctan \left[\frac{\alpha_j \sqrt{\lambda_j} \sin(2y)}{\sqrt{\lambda_j(0)}} \right]. \quad (13)$$

Putting these back in Eq. (6), we obtain the time evolution of the circuit complexity. Before studying this evolution we consider the following special cases.

C. Early time growth and the zero mode contribution

We first study the behaviour of the complexity at $t \rightarrow 0$, i.e., just after the quench. The behaviour of other information theoretic quantities such as the entanglement entropy have been studied previously at this limit. From the expressions in Eq. (13), we see that at $t = 0$, both $\mathcal{A}_j(t = 0) = 0$, $\mathcal{B}_j(t = 0) = 0$, hence at $t = 0$ we have $\mathcal{C}(t = 0) = 0$. Higher order terms in the expansion can be obtained using Eqs. (6) and (7) and are given as $\mathcal{C}^2(t) = a_2 t^2 + a_4 t^4 + \dots$, with

$$a_2 = \frac{1}{4} \sum_{j=1}^N \frac{(\lambda_j - \lambda_j(0))^2}{\lambda_j(0)}, \quad a_4 = \frac{1}{4} \sum_{j=1}^N \frac{(\lambda_j - \lambda_j(0))^2 (5\lambda_j^2 - 6\lambda_j \lambda_j(0) + 5\lambda_j(0)^2)}{12\lambda_j(0)^2}, \quad \dots \quad (14)$$

We note that, similar to the result obtained using the covariance matrices [33], the complexity squared only contains the even powers of time. Thus very close to the initial time, just after the quench, the complexity grows linearly in time (here $a_2 > 0$).

As an alternative limit, we can also calculate the first order contribution to the complexity when the target frequency is only infinitesimally different from the reference frequency, i.e., $\omega_f = \omega_i + \delta$, with $\delta \ll 1$. In this case the $\mathcal{O}(\delta)$ contributions to the functions \mathcal{A}_j and \mathcal{B}_j with $k_f = k_i$ are given by

$$\mathcal{A}_j(\omega_f = \omega_i + \delta) \approx \frac{2\omega_i \sin^2(\sqrt{\lambda_j(0)}t)}{\sqrt{\lambda_j(0)}} \delta + \mathcal{O}(\delta^2), \quad \mathcal{B}_j(\omega_f = \omega_i + \delta) \approx -\frac{\omega_i \sin(2t\sqrt{\lambda_j(0)})}{\sqrt{\lambda_j(0)}} \delta + \mathcal{O}(\delta^2). \quad (15)$$

These two terms contribute at $\mathcal{O}(\delta)$ to the complexity. It can now be seen that when we take the reference frequency to be zero, the complexity does not have any $\mathcal{O}(\delta)$ contribution. This is in contradiction with the results obtained from the covariance method, where there is an $\mathcal{O}(\delta)$ contribution to the complexity in this case. This result indicates that for small change of the reference frequency from the initial zero value, the complexity calculated from the wavefunction cannot detect the lowest order change in the complexity, whereas complexity computed using the covariance matrix shows a linear behaviour, one that is of first order in the target state frequency.

Next, we investigate the contribution of the N -th mode towards the total complexity. As we shall see below, the N -th mode contribution determines the behaviour of the complexity at late times. For the complexity calculated using the covariance matrix method, the contribution of the N -th mode has been investigated in details in [33]. When $\lambda_j \rightarrow 0$, this is the zero mode contribution. Here, our goal is to analyse this contribution with our formula.

The contribution of N -th mode (denoted by \mathcal{C}_0) and the rest can be written as $\mathcal{C}^2(t) = \mathcal{C}_r^2(t) + \mathcal{C}_0^2(t)$, with $\mathcal{C}_r^2(t) = \frac{1}{4} \sum_{j=1}^{N-1} (\mathcal{A}_j^2(t) + \mathcal{B}_j^2(t))$, and $\mathcal{C}_0^2 = \frac{1}{4} (\mathcal{A}_N^2 + \mathcal{B}_N^2)$, i.e.,

$$\mathcal{C}_0^2 = \frac{1}{4} \left(\ln \left[\frac{\sqrt{\alpha_N^2 \lambda_N \sin^2(2y_N) + \lambda_N(0)}}{(\gamma_N + \alpha_N \cos(2y_N)) \sqrt{\lambda_N(0)}} \right] \right)^2 + \frac{1}{4} \left(\arctan \left[\frac{\alpha_N \sqrt{\lambda_N} \sin(2y_N)}{\sqrt{\lambda_N(0)}} \right] \right)^2, \quad (16)$$

where we have denoted $y_N = \sqrt{\lambda_N} t$. With this expression for the N -th mode contribution, we can provide an upper and lower bound to the circuit complexity as $\mathcal{C}_0(t) \leq \mathcal{C}(t) \leq \mathcal{C}_u$, with

$$\mathcal{C}_u^2(t) = \mathcal{C}_0^2(t) + \frac{1}{4} \sum_{j=1}^{N-1} [\mathcal{A}_{uj}^2 + \mathcal{B}_{uj}^2], \quad \mathcal{A}_{uj} = \ln \left[\frac{\sqrt{\alpha_j^2 \lambda_j + \lambda_j(0)}}{\gamma_j \sqrt{\lambda_j(0)}} \right], \quad \mathcal{B}_{uj} = \arctan \left[\frac{\alpha_j \sqrt{\lambda_j}}{\sqrt{\lambda_j(0)}} \right], \quad (17)$$

These bounds will be plotted along the complexities in the plot below to check their validity.

D. Time evolution of complexity : revivals

The time evolution of the complexity after a quench is shown in Fig. (1) when the harmonic chain contains four interacting oscillators, whose interaction strength changes from $k_i = 2$ to $k_f = 2.5$ and the frequency $\omega_i = 3$ is changed to $\omega_f = 0.3, 0.1$ and 0.01 . To make a comparison with plots of von Neumann entropy, we have kept the parameter values the same as in reference [34]. Very similar to the plots of the von Neumann entropy in that work, circuit complexity show revivals during the evolution, and the time period of revival increases as the values of the post-quench frequency is decreased. Furthermore, similar to the von Neumann entropy, complexity also shows quasi-revivals of shorter time period, with these time periods generated dynamically. Furthermore, neither the entanglement entropy, nor the complexity saturates with time.

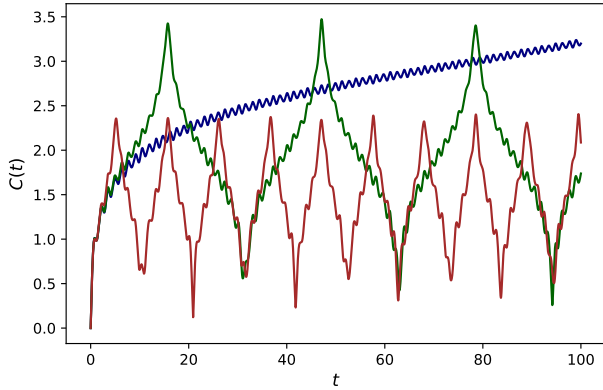


FIG. 1. Time evolution of complexity after a single quench, with the same reference state frequency and different target state frequencies and $N = 4$. The red, green and blue curves are for $\omega_f = 0.3, 0.1, 0.01$, with $k_i = 2, k_f = 2.5, \omega_i = 3$. Dynamically generated time scales can be seen from this plot.

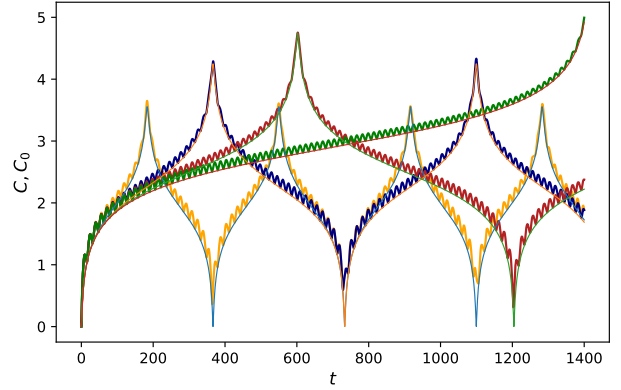


FIG. 2. Time evolution of complexity after a single quench with same reference state frequency and different target state frequencies and $N = 100$. Here, $\omega_i = 0.3$, $k_f = k_i = 10$. The yellow, blue, red and green curves denote $\omega_f = 0.009, 0.004, 0.002, 0.001$. The lower bound in Eq. (16) for each target frequency is also plotted.

There are however, important differences between them as well. For example there are sharp peaks present in the complexity, with the magnitude of these peaks increase with decreasing the value of the final frequency, i.e., as we move away from the initial frequency. These peaks are markedly absent from the plots of the von Neumann entropy. It can be checked that in the expression of Eq. (6) the term $\sum_{j=1}^n \mathcal{A}_j^2$ is responsible for these peaks. On the space of unitary operators these points represent the maximum distance between the target state and the reference state and it is determined by the magnitude of the reference and the target state frequencies rather than their complex phase factors. Furthermore, though complexity has sharp minima, it never reaches zero, i.e., the time evolved state never coincides with the state before quench at $t = 0$.

The time evolution of complexity with a large number of particles is shown in Fig. 2, with particle number $N = 100$. Once again, the plots of the complexity show sharp peaks besides the presence of the dynamically generated time periods of oscillation as well as quasi-revivals. Revivals observed here for the complexity calculated using the wavefunction method is also shared by the complexity obtained from the covariance matrix [33].

In the same figure, we have also plotted the corresponding lower bounds of the complexity given in Eq. (16). For all the target state frequencies, the lower bounds are very useful. The upper bound to the complexity given in Eq. (17) can also be shown to provide excellent consistency, however we have not shown it here, in order not to clutter the diagram.

E. Time evolution after critical quench

Next we shall consider the time evolution of complexity after a critical quench. For the critical evolution, the frequency after the quench vanishes i.e. $\omega_f = 0$. In this limit, the zero mode contribution can be simplified as

$$C_{0c}^2 = \frac{1}{16} \left(\ln [1 + t^2 \omega_i^2] \right)^2 + \frac{1}{4} \left(\arctan [\omega_i t] \right)^2. \quad (18)$$

It can now be seen that, due to presence of the first term in the zero mode, at $t \rightarrow \infty$, the complexity diverges logarithmically (the second term takes a constant value in this limit).

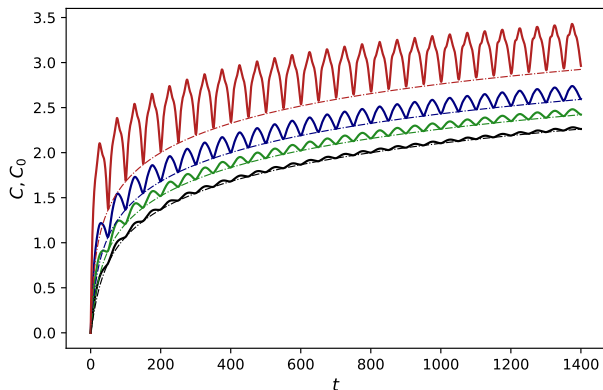


FIG. 3. Time evolution of complexity of after the critical quench with $N = 100$. The black, green, blue and red lines correspond to $\omega_i = 0.05, 0.07, 0.1, 0.2$, with $k_i = k_f = 1$ and $\omega_f = 0$. The lower bound in this case in Eq. (18) is also shown for each reference frequency.

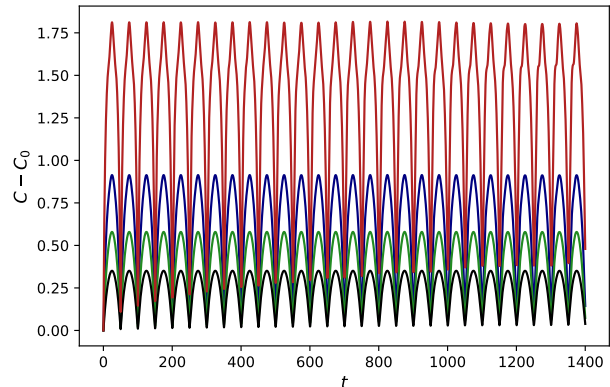


FIG. 4. Time evolution of complexity minus the zero mode contribution for critical quench with the parameter value same as Fig. 3, with the same colour coding. The zero mode is responsible for growth of complexity with time.

Time evolution of circuit complexity after the critical quench for different values of the reference state frequencies are plotted in Fig. 3 with $N = 100$. The lower bounds in Eq. (18) for different reference state are also plotted in the same figure. With increasing reference state frequency, as well as for large times, this bound becomes slightly less reliable. As can be seen from these plots, in contrast to the non-critical cases, for the critical quench, complexity grows with time. This is due to the divergence of the zero mode contribution at large times. To see this more explicitly we have plotted in Fig. 4, corresponding to the complexities plotted in Fig. 3 the total complexity minus the zero mode contribution. When the zero mode is subtracted, the complexity does not increase, and rather oscillates with time.

The growth of the circuit complexity with time for the critical quench is also observed in the complexity calculated using the covariance matrices in [33]. However, in this case, when the zero mode contribution is subtracted from the complexity the resulting expression shows decoherence with time for relatively higher values of the reference state frequency. This is in sharp contrast with our case, where the complexity calculated using the wavefunction does not show such decoherence with time.

III. COMPLEXITY EVOLUTION IN A HARMONIC CHAIN UNDER MULTIPLE QUENCHES

Now we will investigate the time evolution of circuit complexity in the harmonic chain of the previous section, when it is subjected successively to more than one quench. For such multiple quench protocol, the time evolution of entanglement entropy and the out of time order correlator (OTOC) have been recently studied in [16], where marked changes of these quantities from their single quench counterpart are observed.

Our quench protocol is the following. At $t = 0$, the frequency ω_i is changed to ω_f by keeping the other parameter k unchanged. Now, after a time period T , the new frequency ω_f is changed back to the old one ω_i , thereby defining a second quench. This sequence is now repeated to define a multiple quench protocol. For now we shall assume that all the quenches are non-critical in nature. The case when any quench of the sequence is critical will be dealt with later.

The solution for the auxiliary equation for the j th particle after the i th quench of time period T can be written in terms of $y = \sqrt{\lambda_j}t$ as

$$b_{j,i}((i-1)T < t < iT) = \sqrt{A_{j,i} \cos^2 y + 2B_{j,i} \sin y \cos y + C_{j,i} \sin^2 y} = \sqrt{\alpha_{j,i} \cos(2y) + \beta_{j,i} \sin(2y) + \gamma_{j,i}}. \quad (19)$$

Here each of these solutions are valid for their respective range of time period of quench, and hence we need to use the appropriate expression for λ_j , either $\lambda_{(f)j}(t) = \omega_f^2(t) + 2k(t)[1 - \cos(\frac{2\pi j}{N})]$, or $\lambda_{(i)j}(t) = \omega_i^2(t) + 2k(t)[1 - \cos(\frac{2\pi j}{N})]$, depending on the time period under consideration. To determine the constants appearing in the above solutions, we demand that the solutions $b_{j,i}(t)$ and their time derivative $\dot{b}_{j,i}(t)$ are continuous for each value of the index i i.e., after and before a quench their values should match. This two conditions determine two of the above constants and the third can be determined by using the relation (10) between them.¹ Furthermore, at $t = 0$, the conditions at Eq. (5) are valid as well, which (along with Eq. (10)) should determine the constants $A_{j,1}, B_{j,1}, C_{j,1}$. The expressions for the rest of the constants can be obtained in terms of them.

Let us suppose that we have performed n quenches following the protocol discussed above. First, we shall study the time evolution of complexity between a reference state at $t = 0$ and a target state at a time t after the n th quench. The formula for the complexity \mathcal{C}_i between the time interval $(i-1)T < t < iT$ can be written as

$$\mathcal{C}_i^2((i-1)T < t < iT) = \frac{1}{4} \sum_{j=1}^N \left(\mathcal{A}_{j,i}^2(b_{j,i}, \dot{b}_{j,i}) + \mathcal{B}_{j,i}^2(b_{j,i}, \dot{b}_{j,i}) \right), \quad (20)$$

where we have defined

$$\mathcal{A}_{j,i}(t) = \ln \left[\frac{\sqrt{b_{j,i}^2(t) \dot{b}_{j,i}^2(t) + \lambda_{(i/f)j}}}{\sqrt{\lambda_{(i)j} b_{j,i}^2(t)}} \right] \quad \text{and} \quad \mathcal{B}_{j,i}(t) = \arctan \left[\frac{b_{j,i}(t) \dot{b}_{j,i}(t)}{\sqrt{\lambda_{(i)j}}} \right]. \quad (21)$$

Here the notation $\lambda_{(i/f)j}$ represents $\lambda_{(i)j}$ or $\lambda_{(f)j}$ depending on the quench number. Thus the total complexity contains n different parts corresponding to the individual complexities in each section of the quench. Since the quantities \mathcal{C}_i depend on auxiliary functions $b_{j,i}$ and their derivatives, and they are continuous between successive quenches, the complexity at an arbitrary time t is a continuous function.

¹ The relations corresponding to that of Eq. 10 for the second set of constants are given by $\gamma_{j,i}^2 - \beta_{j,i}^2 - \alpha_{j,i}^2 = \lambda_j(0)/\lambda_{(i)j}$ or $\gamma_{j,i}^2 - \beta_{j,i}^2 - \alpha_{j,i}^2 = \lambda_j(0)/\lambda_{(f)j}$ depending on the value of time t .

For the solutions of the auxiliary functions written above, these functions are given by

$$\begin{aligned} \mathcal{A}_{j,i}(t) &= \ln \left[\frac{\sqrt{\lambda_{(i)j} + (\beta_{j,i} \cos(2\sqrt{\lambda_{(i/f)j}t}) - \alpha_{j,i} \sin(2\sqrt{\lambda_{(i/f)j}t}))^2 \lambda_{(i/f)j}}}{(\alpha_{j,i} \cos(2\sqrt{\lambda_{(i/f)j}t}) + \beta_{j,i} \sin(2\sqrt{\lambda_{(i/f)j}t}) + \gamma_{j,i}) \sqrt{\lambda_{(i)j}}} \right], \\ \mathcal{B}_{j,i}(t) &= \arctan \left[\frac{(\alpha_{j,i} \sin(2\sqrt{\lambda_{(i/f)j}t}) - \beta_{j,i} \cos(2\sqrt{\lambda_{(i/f)j}t})) \sqrt{\lambda_{(i/f)j}}}{\sqrt{\lambda_{(i)j}}} \right]. \end{aligned} \quad (22)$$

It can be easily seen that just after the first quench, for a time $t \ll T$ the complexity grows proportional to t , since in this case the evolution of complexity is the same as in a single quench. Similarly, after each quench we can expand the complexity in powers of t , and we obtain the following series (with the time being shifted for the higher quench number) $\mathcal{C}_i^2(t) = a_{i0} + a_{i1}t + a_{i2}t^2 + \dots$, where now the complexity has a finite value at zeroth order in time, given by

$$a_{i0} = \frac{1}{4} \sum_{j=1}^N \left\{ \left(\log \left[\frac{(\alpha_{j,i} + \gamma_{j,i}) \sqrt{\lambda_{(i)j}}}{(1 + \beta_{j,i}^2) \sqrt{\lambda_{(i/f)j}}} \right] \right)^2 + \left(\arctan \left[\frac{\beta_{j,i} \sqrt{\lambda_{(i/f)j}}}{\sqrt{\lambda_{(i)j}}} \right] \right)^2 \right\}. \quad (23)$$

When we consider the first quench this quantity will be zero. In contrast to the single quench the linear growth is now determined by the coefficient of t (a_{i1}) and the zeroth order contribution (a_{i0}).

The zero mode contribution for the multiple quench now consists of n different contributions accounting for n quenches and the contribution of the i th quench can be written as follows

$$\mathcal{C}_{i0}^2 = \frac{1}{4} \left(\mathcal{A}_{N,i}^2(b_{N,i}, \dot{b}_{N,i}) + \mathcal{B}_{N,i}^2(b_{N,i}, \dot{b}_{N,i}) \right). \quad (24)$$

The expressions for the functions $\mathcal{A}_{N,i}^2(b_{N,i}, \dot{b}_{N,i})$ and $\mathcal{B}_{N,i}^2(b_{N,i}, \dot{b}_{N,i})$ can be read from Eqs. (22) above. During the complexity evolution after each quench these provide a lower bound to the complexity in the time period under consideration.

A. Complexity evolution with multiple quenches

Now we shall study the time evolution of the complexity between a reference state at $t = 0$ and a target state at an arbitrary time t numerically by using the formula in Eq. (20) which is valid when the target state is between $(i-1)T < t < iT$. Here we impose a smooth matching between the auxiliary functions and its time derivative at times iT , with $i = 1, 2, \dots, n$ i.e. after and before any particular quench. The values of the first set of constants $\alpha_{j,1}, \beta_{j,1}, \gamma_{j,1}$ can be obtained by imposing the conditions of Eq. (5) at $t = 0$, and they are given by: $\alpha_{j,1} = \frac{\lambda_{(f)j} - \lambda_{(i)j}}{\lambda_{(f)j}}, \beta_{j,1} = 0, \gamma_{j,1} = \frac{\lambda_{(f)j} + \lambda_{(i)j}}{\lambda_{(f)j}}$. By using these values, the continuity of the auxiliary functions and its derivative across each quench and the relation between the three constants mentioned above the other independent constants can be obtained at successive quenches.

In Fig. 5 we have plotted the time evolution of the circuit complexity after five successive quenches between frequency $\omega_i = 3$ and $\omega_f = 5$, with $k_f = k_i = 4$, $T = 4$, for a harmonic chain containing 100 particles. The complexity shows oscillating behaviour, with the magnitude of the oscillations being dependent on the frequency of the chain. From this plots we can make the following observations. ²

² These conclusions are valid for frequency ω_f sufficiently higher than ω_i . We are not considering critical quenches in this section.

Firstly, comparing the complexities of the states having the same frequencies ω_i , we see that among these equal frequency states the state at higher times has higher complexity. Hence even after two successive quenches when we come back to the same frequency ω_i the unitary operator corresponding to this state does not come back to its previous position on the space of unitary operators, rather it further moves away from it. The reason for this behaviour is that, after two quenches, even though the frequency returns to its pre-quench value the solution for the auxiliary function, and hence the wavefunction is necessarily different from their expressions at $t = 0$ due to the inherent time dependence of the problem. Thus there is always some ‘residual’ complexity that is present between two states at $t = 0$ and $t \geq 4$ due to the time dependence of the problem. However, with two successive quenches between frequency ω_f the complexity does come to values same as that of previous quench with the same frequency.

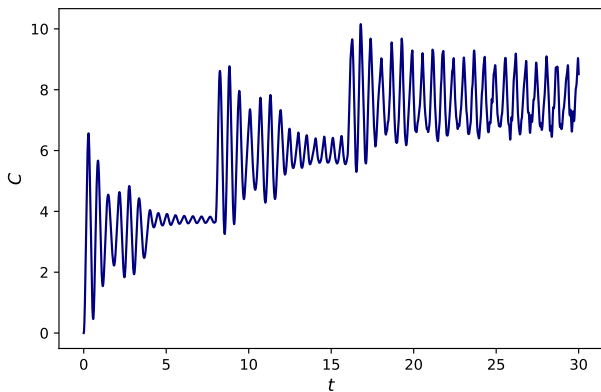


FIG. 5. Time evolution of complexity with five successive quenches with $N = 100$. Here, $k_f = k_i = 4, T = 4, \omega_f = 5$ and $\omega_i = 3$.

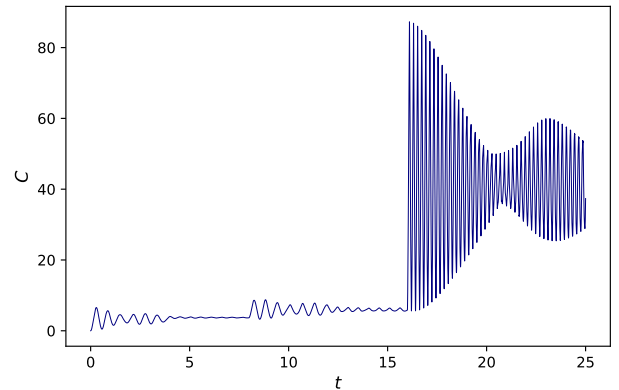


FIG. 6. Time evolution of complexity with five successive quenches when the final quench frequency is much higher than the preceding ones. Here, we set $\omega_f = 5$ after first and third quench, and $\omega_i = 3$ after second and fourth quench. For fifth quench frequency is $\omega_f = 15$.

Secondly, comparing the complexities of the time period of the i th quench with frequency ω_i and that of the $(i + 1)$ th quench, having frequency ω_f we notice that, for sufficiently high value of ω_f compared with the initial frequency, there are times just after the $(i + 1)$ th quench when the complexity evolves to values smaller even than those of the i th quench. These points on the space of unitary operators are closer to the initial state than those of the state with i th reference frequency. Gradually these oscillations dry out slightly so that complexity oscillates around a value higher than that of the previous quench. However even at large times these oscillations do not dry out completely, so that complexity does not attain a steady state value.

In this context an interesting question is the following: since the complexity just after the $(i + 1)$ th quench is smaller than the i th quench, and as we have seen above the magnitude of the oscillations of the complexity depends on the frequency of the quench is it possible to decrease the complexity after the $(i + 1)$ th quench to a value which is much lower than that of the i th quench. In particular is it possible to make the complexity very close to zero, i.e. to made the time evolved state after multiple quenches approach the reference state at $t = 0$ by increasing the magnitude of the quench frequency? We have shown the time evolution of complexity in such an example in Fig.

6, where the final quench frequency is much larger than the other frequencies. It can be seen from this plot, the complexity after the fifth quench does not get lower than a value much smaller than the fourth quench. Thus there is limit how far the time evolved state after a particular quench can reach close to the reference state. This minimum value can not be decreased even by increasing the quench frequency sufficiently.

If we now increase the number of quenches the complexity after the final quench oscillates around increasingly higher values. Thus, after a sufficiently large number of quenches is applied to the system a target state can be prepared with arbitrary large complexity. This is in sharp contrast with the time evolution of the complexity after a single non-critical quench, where the maximum value of the complexity is given by sharp peaks which are fixed ones the targets state frequency is fixed. Hence after the non-critical single quench the unitary operator corresponding to the target state can not go beyond a particular point in the space of unitary operators, whereas after successive quenches the unitary operator can be at a large distance from the identity.

In this context it is important to quantify the differences between the entanglement entropy (EE) of the bipartite system and the circuit complexity. After multiple quenches the complexity does not saturates to any constant value, rather it continue to oscillates around a mean value even at late times. This is in contrast with the behaviour of other information theoretic quantities such as the entanglement entropy. After multiple quenches, compared to the single quench, the entanglement entropy attains a larger steady state value, and higher number of quenches leads to a smaller fluctuation [16]. For the complexity the higher number of quenches can not reduce its fluctuation. On the other hand the non trivial nature of the system after multiple quenches can be also infrared from the fact that in single quench scenario, the CC for various systems is known to saturate after initial linear growth, which in some cases even faster compared to the saturation of EE. This is ones again in contrast with the case considered here.

B. Evolution when the final quench is a critical quench

Now we shall discuss a special case of the multiple quench protocol, namely, when the final n th quench is a critical quench discussed in the context of a single quench in section II E. As we have seen the complexity in this case grows with time due to the logarithmic divergence of the zero mode contribution towards the total complexity.

In Fig. 7, we have plotted the time evolution of the circuit complexity with three (red curve) and five quenches (blue curve) when the when the final quench is a critical quench. In both the plots after the characteristic oscillatory behaviour of the complexity under the non-critical quench the the complexity shows linear growth which is characteristic of the critical quench. However due to the fact that the final quench is a critical quench now there is a discontinuity in the complexity at the final quench which is markedly absent from the non-critical multiple quench plots. This discontinuity in the complexity is due to the discontinuity in the N -th mode contributions for non-critical and critical quenches. As we have seen before at the limit of critical quench the zero mode contribution attains a particular value given by Eq. (18) which is different from the non-critical contributions in Eq. (16).

To see this clearly we have plotted the N -th mode contribution separately in Fig. 8, where the discontinuity at the critical quench is visible in both the case of three and five quenches.

In both the Figures 7 and 8 the derivatives of the complexity and the zero mode contribution are also shown separately which make the discontinuity of these quantities at the critical quench clearly visible.

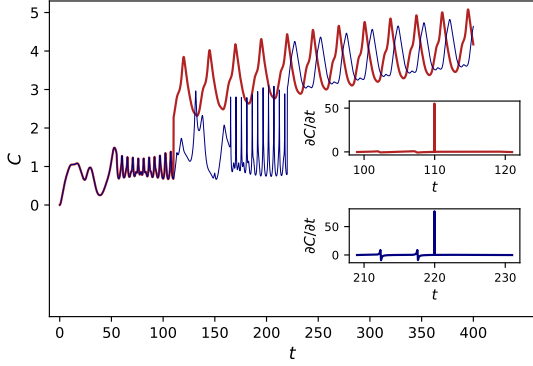


FIG. 7. Time evolution of complexity with three (Red) and five (Blue) successive quenches when the final quench is critical quench. Here, $\omega_i = 0.3, \omega_f = 0.085$ (when non-critical), $K_i = k_f = 4$ and $T = 55$. There is a discontinuity after the critical quench, which is evident from the plots of the derivatives of the complexity shown separately for two cases in the inset.

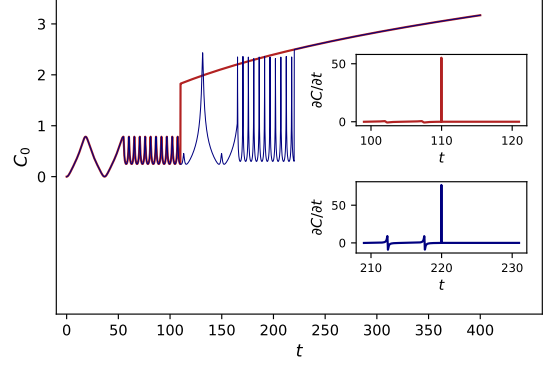


FIG. 8. N -th mode contributions corresponding to Fig. 7. There is a discontinuity after the critical quench. The derivatives of the zero mode contribution are shown separately for two cases in the inset, from which the discontinuity is clearly seen.

C. Complexity between states of subsequent quenches

So far we have calculated the circuit complexity between states at $t = 0$ and an arbitrary time evolved state after a single or multiple quenches. For more than one quenches we can calculate another set of quantities which is not possible in the case of a single quench, namely the complexity between states of successive quenches, namely the complexity between a state before and after a particular quench, so that the reference state is not the state at initial time. These quantities will provide us with important information regarding the change of complexity after each quench which are not captured when the reference state is a fixed state before the first quench.

As an example of calculation of such quantity let us compute the circuit complexity between a reference state at a time $t = t_0$ of the i th quench and a target state at an arbitrary time t between $t_0 < t < (i+1)T$. This quantity will help us to quantify the exact change of the complexity between different quenches. The expression for the complexity between time period $iT < t < (i+1)T$ can be written as [28]: $C_s(t) = \frac{1}{2} \sqrt{\sum_{j=1}^N (\mathcal{A}_{sj}^2 + \mathcal{B}_{sj}^2)}$, where \mathcal{A}_{sj}^2 and \mathcal{B}_{sj}^2 are functions of $b_{j,i}(t_0), \dot{b}_{j,i}(t_0), b_{j,i+1}, \dot{b}_{j,i+1}$, and are given by

$$\mathcal{A}_{sj}(t) = \ln \left[\frac{|\Omega_{Tj}|}{|\Omega_{Rj}|} \right], \quad \mathcal{B}_{sj}(t) = \arctan \left[\frac{\text{Im}(\Omega_{Tj})\text{Re}(\Omega_{Rj}) - \text{Im}(\Omega_{Rj})\text{Re}(\Omega_{Tj})}{\text{Re}(\Omega_{Rj})\text{Re}(\Omega_{Tj}) + \text{Im}(\Omega_{Rj})\text{Im}(\Omega_{Tj})} \right]. \quad (25)$$

Here, Ω_{Tj} is the complex frequency of the target Gaussian state, of the form of Ω_j given in Eq. (3), and Ω_{Rj} is the frequency of reference state: $\Omega_{Rj} = \Omega_j(t_0)$, where $iT < t < (i+1)T$ and $(i-1)T < t_0 < iT$ is a fixed value of time at

i th quench. The expressions for these functions $\mathcal{A}_{sj}(t)$ and $\mathcal{B}_{sj}(t)$ can be written in terms of the auxiliary function $b_{j,i}(t_0)$ and $b_{j,i+1}(t)$ and their derivative as

$$\mathcal{A}_{sj}(iT < t < (i+1)T) = \ln \left[\frac{b_{j,i}^2(t_0) \sqrt{b_{j,i+1}^2(t) \dot{b}_{j,i+1}^2(t) + \lambda_{(i/f)j}}}{b_{j,i+1}^2(t) \sqrt{b_{j,i}^2(t_0) \dot{b}_{j,i}^2(t_0) + \lambda_{(f/i)j}}} \right], \quad (26)$$

and

$$\mathcal{B}_{sj}(iT < t < (i+1)T) = \arctan \left[\frac{b_{j,i}(t_0) \dot{b}_{j,i}(t_0) \sqrt{\lambda_{(f/i)j}} - b_{j,i+1}(t) \dot{b}_{j,i+1}(t) \sqrt{\lambda_{(i/f)j}}}{\sqrt{\lambda_{(i/f)j}} \sqrt{\lambda_{(f/i)j}} + b_{j,i}(t_0) \dot{b}_{j,i}(t_0) b_{j,i+1}(t) \dot{b}_{j,i+1}(t)} \right]. \quad (27)$$

Note that here $b_{j,i}(t_0)$ and $\dot{b}_{j,i}(t_0)$ are constants, indicating the value of the auxiliary function $b_{j,i}(t)$ and its derivative at a time t_0 . Furthermore, during the time period $t_0 < t < iT$, i.e. between time t_0 and that of the i th quench the expression for the complexity is given by a similar formula as that of above with with $b_{j,i+1}(t)$ and $\dot{b}_{j,i+1}(t)$ respectively replaced by the auxiliary function $b_{j,i}(t)$ and its derivative respectively. Thus the functions \mathcal{A}_{sj} and \mathcal{B}_{sj} in this case are given by

$$\mathcal{A}_{sj}(t_0 < t < iT) = \ln \left[\frac{b_{j,i}^2(t_0) \sqrt{b_{j,i}^2(t) \dot{b}_{j,i}^2(t) + \lambda_{(i/f)j}}}{b_{j,i}^2(t) \sqrt{b_{j,i}^2(t_0) \dot{b}_{j,i}^2(t_0) + \lambda_{(i/f)j}}} \right], \quad (28)$$

and

$$\mathcal{B}_{sj}(t_0 < t < iT) = \arctan \left[\frac{b_{j,i}(t_0) \dot{b}_{j,i}(t_0) \sqrt{\lambda_{(i/f)j}} - b_{j,i}(t) \dot{b}_{j,i}(t) \sqrt{\lambda_{(i/f)j}}}{\sqrt{\lambda_{(i/f)j}} \sqrt{\lambda_{(i/f)j}} + b_{j,i}(t_0) \dot{b}_{j,i}(t_0) b_{j,i}(t) \dot{b}_{j,i}(t)} \right]. \quad (29)$$

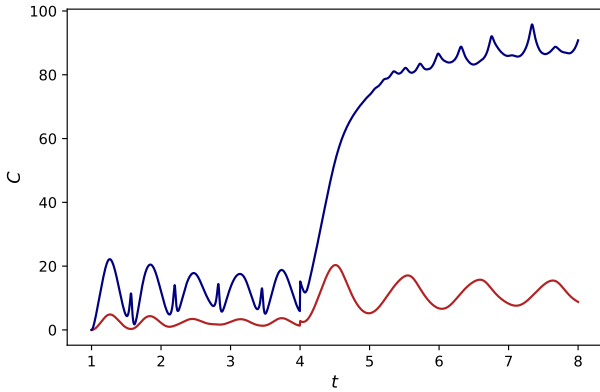


FIG. 9. Time evolution of complexity between first and second quench, with $N = 100$ and $k_f = k_i = 4, T = 4$. Blue: $\omega_f = 5$ and $\omega_i = 0.3$, red: $\omega_i = 3$ and $\omega_f = 5$.

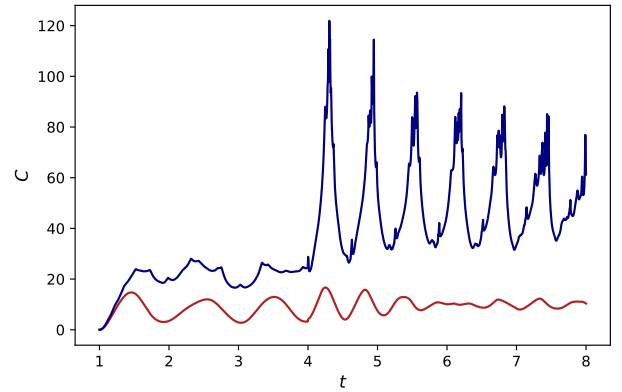


FIG. 10. Time evolution of complexity between second and third quench, with $N = 100$ and $k_f = k_i = 4, T = 4$. Blue: $\omega_f = 5$ and $\omega_i = 0.3$, red: $\omega_i = 3$ and $\omega_f = 5$.

Time evolution of complexity between the first and second quenches is shown in Fig. 9, and between the second and third quenches is shown in Fig. 10, with Fig. 10 being shifted appropriately in time. In Fig. 9, the reference state is chosen to be a state at fixed time $t_0 = 1$ after the first quench and the target state is a state at an arbitrary time t between $t_0 < t < 2T$ where $T = 4$. While in Fig. 10, the reference state is taken at $t_0 = 5$, just after the second quench and the target state is a state is between $t_0 = 5 < t < 3T$. In both the cases the blue curve is with $\omega_i = 0.3, \omega_f = 5$ and the red one with $\omega_i = 3, \omega_f = 5$.

The first point to note is that in both the cases, just after the $i + 1$ th quench, there is a sharp rise in the complexity, which was absent when the complexity was calculated from the fixed state before the quench. When the difference between the target state and reference state frequencies are higher, the growth of the complexity after the quench is sharper. This growth can be characterised by expanding the complexity in Eq. (25) in powers of t as in Eq. (23) and finding out the coefficients of various order contributions.

As we have mentioned before, when the reference state is a fixed at $t = 0$, for a time period just after any quench, say with a quench number i , the complexity has value lower than its value at $t < (i - 1)T$. For example, we see from Fig. 5 that after the second quench (where $t = 8$) the complexity increases and then takes a value lower than its value at $t = 8$. However, unlike in Fig. 5, here, for the complexity between states in successive quenches, the complexity never comes below its pre-quench value. Thus when the reference state is a state in the i th quench and the target state is in the $(i + 1)$ th quench, during the evolution after the $(i + 1)$ th quench, the target state never comes closer to the reference state than the state during i th quench. Thus after the quench complexity sharply increases. This is in sharp contrast with the complexity evolution the with reference state before the quench.

Another interesting phenomena can be observed by comparing the complexities between two different successive quenches. In Fig. 11, we have compared the complexities between the first and the second quench (red curve) to that of between the third and the fourth quench (blue curve). Here, the time scale of the blue curve has been shifted to make a comparison. Comparing these two curves, we see that before the $i + 1$ th quench ($i = 1$ for red and $i = 3$ for blue), the complexity with higher value of i is always higher. However just after the $i + 1$ th quench is performed, the complexity having lower value of i crosses the complexity with higher i and always stays higher up to their respective ranges of time. In terms of points on the space of unitary operators, we can interpret this phenomena

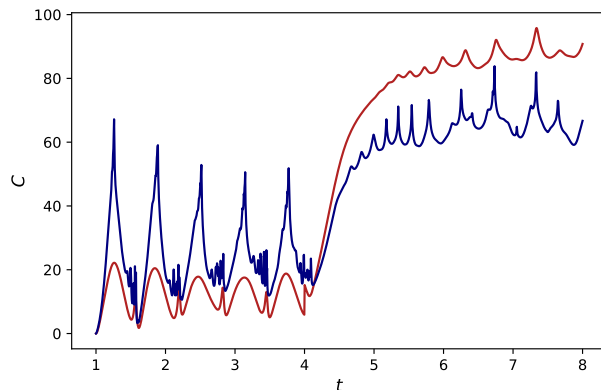


FIG. 11. Comparison of complexities between first and second quench (red curve), with that of third and fourth quench (blue), with $N = 100$, $k_f = k_i = 4$, $T = 4$, $\omega_f = 5$ and $\omega_i = 0.3$.

as follows. Let us take the states at two different t_0 s on two i th quenches to be two fixed reference states on the unitary manifold and compute the distances of two time evolved states before the respective $(i + 2)$ th quenches from these two reference states. Before the $(i + 1)$ th quenches are performed the target state which is located at later

times is always at a further distance from its reference state than the one at earlier time. But ones the $(i + 1)$ th quench is performed this distance changes rapidly so that the target state at higher time comes much closer to its reference state than the one at lower time. Thus we can conclude that the effect a quench at an earlier time is to ‘push away’ the time evolved state on the space of unitary manifold compared with a target state at a later time. This phenomena can not be observed when a single quench is performed on the harmonic chain.

We also notice that this ‘crossover’ of the complexities of successive quenches can be most clearly observed when the frequency ω_f is sufficiently higher than the initial frequency ω_i . For these two frequencies having a value much closer to each other, the behaviour of complexity evolution is more intricate and it will be interesting to quantify this further. Furthermore, it will be interesting to see if this phenomena can be observed in complexity between successive quenches when the covariance matrix is used to calculate the complexity instead of the wavefunction method that we have used. This might be helpful to distinguish these two methods further.

IV. CONCLUSIONS

We have used the Lewis-Risenfeld method to obtain the time evolution of the circuit complexity in a time-dependent harmonic chain under sudden single or multiple quenches of the frequency and coupling strength. Under a single quench, much like the entanglement entropy, the complexity shows quasi-revivals due to the present of dynamically generated time scales, whose number in turn depends on the total number of particles in the chain. When the quench is critical, the complexity grows at large times due to the presence of a zero mode, however it does not show any kind of decoherence in time, even for large post-quench frequency.

On the other hand, when multiple quenches are applied to the chain, though the complexity increases sharply after each quench, however even at late times it does not acquire any steady state value, which is observed in the OTOC - indicating scrambling of information in the chain. For multiple quenches, several new features in the complexity are observed, which can not seen in the single quench scenario. Firstly, even after two successive quenches, when the frequency return to its initial value, there is a lower limit in the value the complexity can have, which cannot be made to approach zero even by increasing the frequency sufficiently. Secondly, by applying a large number of successive quenches to the chain, the complexity of the time evolved state can be increased to a high value, which is not possible by applying a single quench. Finally, the complexity calculated between successive quenched states, having sufficient difference in frequency shows an interesting behaviour, namely, a quench performed at an earlier time (say with a quench number i) ‘pushes away’ the time evolved target state further on the space of unitaries compared to a quench performed at a later time. Thus we observe a crossover of the two complexities just after the $(i + 1)$ th quench.

In this paper, although our analysis is for a sudden quench, the formalism can be applied to more general time-dependent frequencies or interaction profiles, to study the time-evolution of complexity. Furthermore, it will be interesting see weather the special features of the complexity after multiple quenches listed above are shared by

other systems as well.

- [1] A. Polkovnikov, K. Sengupta, A. Silva and M. Vengalattore, *Rev. Mod. Phys.* **83**, 863 (2011).
- [2] L. D'Alessio, Y. Kafri, A. Polkovnikov and M. Rigol, "thermodynamics," *Adv. Phys.* **65**, no.3, 239-362 (2016).
- [3] I. Peschel, *J. Stat. Mech.* (2004) P06004.
- [4] I. Peschel and V. Eisler, *J. Phys. A: Math. Theor.* **42**, 504003 (2009).
- [5] P. Calabrese, F. H. L. Essler, and M. Fagotti, *J. Stat. Mech.* (2012) P07016.
- [6] V. Alba and P. Calabrese, *Phys. Rev. B* **100**, no.11, 115150 (2019).
- [7] A. Larkin and Yu. N. Ovchinnikov, *Zh. Eksp. Teor. Fiz.* **55**, 2262 (1969) [*Sov. Phys, JETP* **28**, 1200 (1969)].
- [8] J. Maldacena, S. H. Shenker and D. Stanford, *JHEP* **08**, 106 (2016).
- [9] K. Hashimoto, K. B. Huh, K. Y. Kim and R. Watanabe, *JHEP* **11**, 068 (2020).
- [10] A. M. Green, A. Elben, C. H. Alderete, L. K. Joshi, N. H. Nguyen, T. V. Zache, Y. Zhu, B. Sundar and N. M. Linke, *Phys. Rev. Lett.* **128**, no.14, 14 (2022).
- [11] N. Roy and A. Sharma, *J. Phys. Condens. Matter* **33**, no.33, 334001 (2021).
- [12] P. V. Buividovich, arXiv:2205.09704 [hep-th].
- [13] R. K. Shukla, A. Lakshminarayan and S. K. Mishra, arXiv:2203.05494 [quant-ph].
- [14] C. J. Lin and O. I. Motrunich, *Phys. Rev. B* **97**, no.14, 144304 (2018).
- [15] T. Xu, T. Scaffidi and X. Cao, *Phys. Rev. Lett.* **124**, no.14, 140602 (2020).
- [16] S. Ghosh , K. S. Gupta and S. C. L. Srivastava, *Phys. Rev. E*, **100** (2019) 012215.
- [17] M. A. Nielsen, arXiv:quant-ph/0502070 [quant-ph].
- [18] M. A. Nielsen, M. R. Dowling, M. Gu, and A. M. Doherty, *Science* **311** (2006) 1133.
- [19] M. A. Nielsen and M. R. Dowling, arXiv:quant-ph/0701004 [quant-ph].
- [20] R. Jefferson and R. C. Myers, *JHEP* **1710**, 107 (2017).
- [21] A. Bhattacharyya, A. Shekar, and A. Sinha, *JHEP* **10**, 140 (2018).
- [22] M. Guo, J. Hernandez, R. C. Myers and S. M. Ruan, *JHEP* **1810**, 011 (2018).
- [23] R. Khan, C. Krishnan, and S. Sharma, *Phys. Rev. D* **98**, 126001 (2018).
- [24] L. Hackl, and R. C. Myers *JHEP* **07** (2018), 139.
- [25] D. W. F. Alves and G. Camilo, *JHEP* **06**, 029 (2018).
- [26] H.A. Camargo, P. Caputa, D. Das, M.P. Heller and R. Jefferson, *Phys. Rev. Lett* **122** (2019), 081601.
- [27] S. Liu, *JHEP* **07** (2019) 104.
- [28] T. Ali, A. Bhattacharyya, S.S. Haque, E.H. Kim, and N. Moynihan, *JHEP.* **04** (2019) 087.
- [29] T. Ali, A. Bhattacharyya, S. S. Haque, E. H. Kim, N. Moynihan and J. Murugan, *Phys. Rev. D* **101**, no.2, 026021 (2020).
- [30] L. C. Qu, J. Chen and Y. X. Liu, arXiv:2111.07351 [hep-th].
- [31] T. Ali, A. Bhattacharyya, S. Shajidul Haque, E. H. Kim and N. Moynihan, *Phys. Lett. B* **811**, 135919 (2020).
- [32] G. Di Giulio and E. Tonni, *JHEP* **12** (2020) 101.
- [33] G. Di Giulio and E. Tonni, *JHEP* **05** (2021) 022.
- [34] S. Ghosh , K. S. Gupta and S. C. L. Srivastava, *Euro. Phys. Lett*, **120** (2017) 50005.
- [35] K. Pal, K. Pal and T. Sarkar, arXiv:2204.06354 [quant-ph].
- [36] S. Mahesh Chandran, S. Shankaranarayanan, arXiv:2205.13338 [hep-th].